Experimental estimation of the heat energy dissipated in a volume surrounding the tip of a fatigue crack

G. Meneghetti (http://orcid.org/0000-0002-3517-9464)
M. Ricotta (http://orcid.org/0000-0002-4212-2618)
University of Padova, Department of Industrial Engineering, Italy
giovanni.meneghetti@unipd.it, mauro.ricotta@unipd.it

ABSTRACT. Fatigue crack initiation and propagation involve plastic strains that require some work to be done on the material. Most of this irreversible energy is dissipated as heat and consequently the material temperature increases. The heat being an indicator of the intense plastic strains occurring at the tip of a propagating fatigue crack, when combined with the Neuber's structural volume concept, it might be used as an experimentally measurable parameter to assess the fatigue damage accumulation rate of cracked components. On the basis of a theoretical model published previously, in this work the heat energy dissipated in a volume surrounding the crack tip is estimated experimentally on the basis of the radial temperature profiles measured by means of an infrared camera. The definition of the structural volume in a fatigue sense is beyond the scope of the present paper. The experimental crack propagation tests were carried out on hot-rolled, 6-mm-thick AISI 304L stainless steel specimens subject to completely reversed axial fatigue loading.

KEYWORDS. Crack tip; Crack propagation; Heat energy; AISI 304L; Averaging approaches.

INTRODUCTION

Numerical or experimental evaluation of plastic dissipation at the tip of fatigue cracks have attracted the attention of several researchers, who investigated, just as few examples, crack propagation assessment criteria [1,2], the thermal effects on stress intensity factors [3,4], the plastic zone size and energy dissipation [5-7]. In the field of the experimental approaches, the development of infrared cameras having increased performances (for example in terms of thermal sensitivity, spatial resolution and frame rate) has given impulse to temperature-related fatigue studies. In a previous paper, dealing with fatigue assessment of notches, the heat energy dissipated in a unit volume of material per cycle, Q, has been assumed as a fatigue damage index and a proper experimental procedure has been put forward to estimate the Q parameter at any point of a specimen or a component undergoing fatigue loadings [8]. Such experimental technique is based on temperature measurements performed by means of an infrared camera or a thermocouple glued at the point of a component where the fatigue assessment is to be performed and it has the advantage that thermal boundary conditions do not need to be controlled during experimental tests. The Q parameter has been applied to correlate fatigue test results obtained on smooth and bluntly notched specimens made of an AISI 304L stainless steel subjected either to constant amplitude [9,10] and two load level [11] fatigue tests. Being a point-related quantity, Q can hardly correlate fatigue test results generated from severely notched specimens, because the well known notch support effect makes questionable the use of peak quantities (stress-, strain- or energy-based) evaluated at the notch tip in order to assess fatigue life. In particular, the use of peak quantities evaluated at the apex of stress concentrators fails by a large amount in the case of fatigue cracks. To account for the notch support effect, Peterson postulated that the controlling factor is the stress at the distance of the structural size ahead the notch tip [12]; on the other hand, Neuber introduced the structural volume concept, inside which stresses are to be averaged [13]. In view of the extension of the heat energy-based approach to severely notched specimens, a theoretical frame and an experimental procedure have been established in the present paper, by considering a specimen containing a propagating fatigue crack. In particular, the specific heat loss Q has been averaged over a volume V surrounding the tip of the propagating crack, leading to the definition of the averaged energy parameter Q*. The volume V, even though on the order of the size of the structural volume for construction steels, has been chosen arbitrarily, since the focus of the present paper is the thermal problem and not yet the validation of a fatigue assessment method. Q* has been estimated starting from the temperature field measured close to the fatigue crack tip. Experimental temperature distributions have been compared with an analytical solution available in the literature.

THEORETICAL BACKGROUND

In order to derive the energy per cycle dissipated in a volume V surrounding a crack tip, a previous theoretical model [8] has been adopted. Let us consider a material undergoing a fatigue test and consider a control volume V surrounding the crack tip, as shown in Fig. 1. The external surface S of the control volume V can be divided into three parts, namely S_{cv}, S_{cd} and S_{ir} through which the heat Q is transferred to the surroundings by convection, conduction and radiation, respectively. The first law of thermodynamics states:

$$\int_V W \cdot dV = \int_V (Q + \Delta U) \cdot dV \tag{1}$$

where W is the input mechanical energy and ΔU the variation of the internal energy. All quantities are referred to a unit volume of material per cycle. Eq. (1) can be written in terms of mean power exchanged over one loading cycle as:

$$\int_V \left(\oint \sigma_{ij} \cdot d\varepsilon_{ij} \right) \cdot f_L \cdot dV = \int_V H \cdot dV + \int_V \left(\rho \cdot c \cdot \frac{\partial T_m}{\partial t} + \dot{E}_p \right) \cdot dV \tag{2}$$

where f_L is the frequency of the applied mechanical load, $H=H_{cd}+H_{cv}+H_{ir}$ is the thermal power dissipated by conduction, convention and radiation, respectively, ρ the material density, c the specific heat and $\dot{E}_p$ the rate of accumulation of damaging energy in a unit volume of material. Let us consider a plane problem and assume that the temperature of a material undergoing a constant amplitude, sinusoidal fatigue loading is given by:

$$T(r,\theta;t) = T_a(r,\theta) \cdot sen\left(2\pi f_L \cdot t\right) + T_m(r,\theta;t) \tag{3}$$

where T_a is the amplitude of temperature oscillations due to the thermoelastic effect and T_m is the mean temperature evolution. T_a and T_m depend on the position (r,θ) considered in the component. It is worth noting that the thermoelastic effect consists of a reversible exchange between mechanical and thermal energy, that does not produce a net energy dissipation or absorption over one loading cycle [14-17]. Since Eq. (2) considers the rate of energy contributions averaged over one cycle, then only the mean temperature evolution $T_m(t)$ appears on the right hand side of Eq. (2).
The specific net heat generation H_{gen} is given by:

$$H_{gen} = \left(\oint \sigma_{ij} \cdot d\varepsilon_{ij} \right) \cdot f_L - \dot{E}_p \tag{4}$$

Therefore Eq. (2) can be written in order to put into evidence only the thermal problem:

$$\int_V H_{gen} \cdot dV = \int_V H \cdot dV + \int_V \rho \cdot c \cdot \frac{\partial T_m}{\partial t} \cdot dV \tag{5}$$

Typically, the mean temperature T_m increases at the beginning of a fatigue tests and, after some time, it stabilises as soon as thermal equilibrium is reached with the surroundings. At thermal stabilisation, T_m is constant with time, therefore the last term on the right hand side of Eq. (5) disappears. As it will be demonstrated later on, H_{cd} can be supposed much greater than H_{cv} and H_{ir}, therefore it can be assumed $H \cong H_{cd}$. The thermal power extracted from volume V of Fig. 1 by conduction can be calculated starting from the thermal flux through its boundary:

$$\int_V H \cdot dV \cong \int_{S_{cd}} -\lambda \cdot grad\vec{T}_m \cdot \vec{n} \cdot dS_{cd} \rightarrow = -\lambda \cdot z \cdot \mathrm{R} \cdot \int_{-\pi}^{+\pi} \left. \frac{\partial T_m(r,\theta)}{\partial r} \right|_{r=\mathrm{R}} \cdot d\theta \qquad (6)$$

where $gradT_m$ is the gradient of the temperature field $T(r,\theta)$, λ is the material thermal conductivity, z is the specimen's constant thickness, $dS_{cd}=z \cdot ds$ (see Fig. 1) and R the radius of the circular volume shown in Fig. 1. In Eq. (6), $h = -\lambda \cdot grad\vec{T}_m \cdot \vec{n}$ is the specific thermal flux evaluated at the point (R,θ) of the boundary of V.

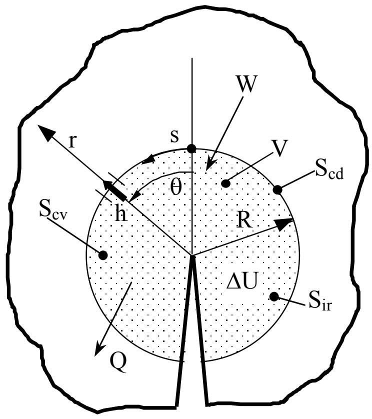

Figure 1: Energy balance for a volume of material V surrounding a crack tip subject to fatigue loadings.

After having calculated the thermal power dissipated by conduction by means of Eq. (6), it is possible to estimate the energy per cycle averaged in the volume V:

$$Q^* = \frac{1}{f_L V} \cdot \int_V H \cdot dV \qquad (7a)$$

Making use of Eq. (6), it is obtained:

$$Q^* = -\frac{1}{f_L V} \cdot \lambda \cdot z \cdot \mathrm{R} \cdot \int_{-\pi}^{+\pi} \left. \frac{\partial T_m(r,\theta)}{\partial r} \right|_{r=\mathrm{R}} \cdot d\theta \qquad (7b)$$

In previous papers, the specific heat loss $Q=H/f_L$ was used as a fatigue damage indicator to perform fatigue assessments [8-11]. Being a point-related quantity, its use was limited to the analysis of the fatigue strength of bluntly notched specimens. Following Neuber's structural volume concept [13], in the present paper the energy term Q is averaged over a control volume V according to Eq. (7), in view of the application of the energy-based approach to severely notched or cracked components. However, it should be noted that the aim of the present paper is to formulate the fatigue related thermal problem and validate an approach able to estimate experimentally Q*. Therefore, the control volume surrounding the crack tip of Fig. 1 was fixed arbitrarily and has not a precise relation to the fatigue properties of the material.
As it will be shown later on, in order to apply Eq. (7b) the surface material temperature was monitored by means of an infrared camera operating at a sample frequency f_{acq}. In order to estimate $T_m(r,\theta)$ at a given time t_s during the fatigue test, a trigger signal was given to the infrared camera at $t=t_s$ and a number of infrared images n_{max} were acquired with a sampling rate f_{acq}. By recalling Eq. (3), the mean temperature field was estimated as pixel-by-pixel average value:

$$T_{m,estimate} = \frac{\sum_{n=1}^{n_{max}} \left\{ T_a \cdot sen\left[2\pi f_L \left(t_s + (n-1)/f_{acq} \right) \right] + T_m \right\}}{n_{max}} \tag{8a}$$

$$T_{m,estimate} = \frac{T_a \sum_{n=1}^{n_{max}} sen\left[2\pi f_L \left(t_s + (n-1)/f_{acq} \right) \right]}{n_{max}} + \frac{T_m \cdot n_{max}}{n_{max}} \tag{8b}$$

where t_s is the time when the temperature acquisition starts. A error index can be defined between the estimated ($T_{m,estimate}$) and the actual (T_m) mean temperature field:

$$\frac{\left| T_{m,estimate} - T_m \right|}{T_a} = \delta \tag{9}$$

By using Eq. (8b) into Eq. (9), the error index results:

$$\left| \frac{\sum_{n=1}^{n_{max}} sen\left[2\pi f_L \left(t_s + (n-1)/f_{acq} \right) \right]}{n_{max}} \right| = \delta \tag{10}$$

Eq. (10) says that for typical testing conditions adopted in the present work, i.e. f_L=37Hz, f_{acq}=200Hz, n_{max}=1000, the relative error δ in the estimation of the mean temperature is lower than 0.1%.

MATERIAL, SPECIMENS' GEOMETRY AND TEST PROCEDURE

Single edge V-notched specimens were machined from a 6-mm-thick hot rolled AISI 304L stainless steel plate (elastic modulus E=194700 MPa, engineering proof stress $R_{p0.2}$=327 MPa, engineering tensile strength R_m=690 MPa [9]), according to the geometry shown in Fig. 2. Constant amplitude, push-pull stress-controlled fatigue tests were carried out by using a servo-hydraulic Schenck Hydropuls PSA 100 machine equipped with a 100 kN load cell and a Trio Sistemi RT3 digital controller. Load test frequencies between 30 and 37 Hz were adopted. Crack propagation was monitored by using a travelling optical stereo-macroscope operating with a magnification of 40x. The material surface temperature was monitored by means of a FLIR SC7600 infrared camera, having a 1.5-5.1 μm spectral response range, 50 mm focal lens, a noise equivalent temperature difference (NETD) < 25 mK, an overall accuracy of 0.05°C, operating at a frame rate, f_{acq}, equal to 200 Hz and equipped with an analog input interface, that was used to sample synchronously the force signal coming from the load cell. The infrared camera and the travelling microscope monitored the opposite surfaces of the specimens, respectively. To increase the infrared camera spatial resolution, a 30 mm extender ring was adopted, which allowed a spatial resolution ranging from 20 to 23 μm/pixel, depending on the distance between the specimen's surface and the focal lens. Due to the extender ring, the Field of View (FoV) was reduced to 320x256 pixels, which corresponds to a minimum of 6.4 mm x 5.1 mm and a maximum of 7.4 mm x 5.9 mm. The specimens' surface were polished by using progressively finer emery papers, namely starting from grade 100 up to grade 1000, and after that the surface was polished with a diamond abrasive powder. Finally, a black paint was applied to the specimens' surface to increase the emissivity.

The acquired temperature maps were processed first by using the FLIR MotionByInterpolation tool to correct the relative motion between the fixed camera lens and the moving specimen subject to cyclic loads, whose displacements ranged from 6 to 14 pixels, depending on the crack length. The infrared images were analysed by means of the dedicated ALTAIR 5.90.002 software, in order to calculate the mean temperature distribution $T_m(r,\theta)$ at a given time $t=t_s$ during the fatigue test according to Eq. (8a). By using Eq. (10), being typically f_L=37 Hz, n_{max}=1000, f_{acq}=200Hz and 0< t_s < 0.5/f_L, it is obtained $\delta \leq 10^{-3}$; such a reduced error was considered acceptable from an engineering point of view. After having determined the distribution of the mean temperature $T_m(r,\theta)$, the heat power dissipated by conduction was calculated by solving Eq. (6) numerically on the basis of a finite number of radial temperature profiles: in particular, 7 radial paths were considered emanating from the crack tip at different θ angles (see Fig. 1), namely 0°, 45°, 90°, 135°, -45°,-90° and-135°. In the present paper, the radius R of the volume surrounding the crack tip was assumed equal to $3\cdot10^{-4}$ m. Even though such a radius may be on the order of the Neuber's structural volume size of a construction steel, it has been assumed as a pure reference example in the present paper, in order to demonstrate the applicability of the proposed approach.

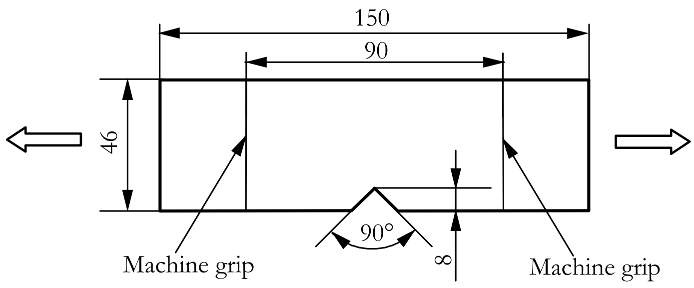

Figure 2: Specimens' geometry (thickness 6 mm).

FATIGUE TEST RESULTS AND TEMPERATURE PROFILES CLOSE TO THE CRACK TIP

Three specimens were tested and the relevant crack growth data are shown in Fig. 3. Linear elastic, two-dimensional, plane stress finite element analyses were performed to evaluate the Mode I stress intensity factor range, $\Delta K=K_{max}-K_{min}$, for different crack lengths. To account for the machine grip effect, displacements were applied in the numerical model to the lines shown in Fig. 2. The Paris curve relating the crack growth rate to ΔK was evaluated and plotted in Fig. 3b.

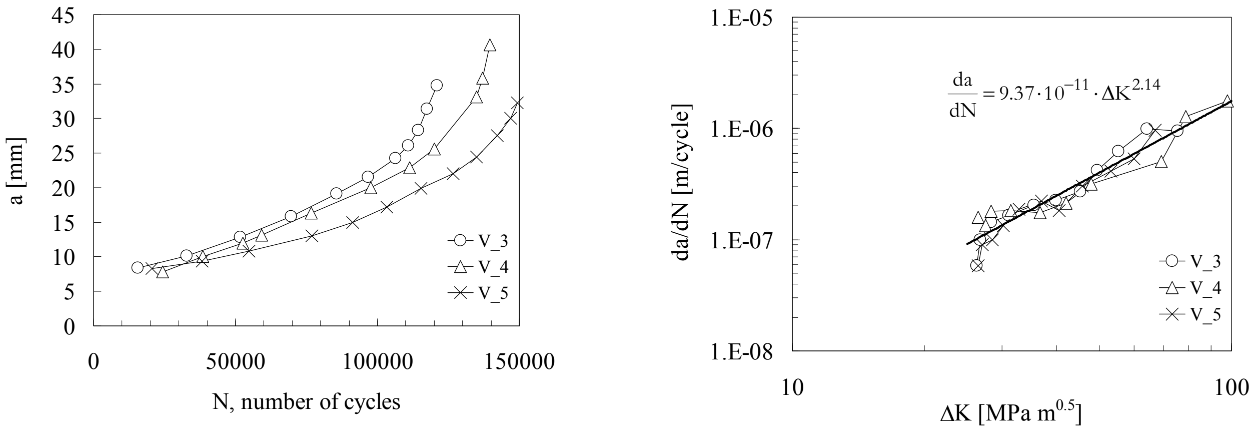

Figure 3: Tension-compression a) crack propagation curves and b) Paris curve of AISI 304 L stainless steel specimens.

The crack length and the temperature field at different ΔK values were measured at several times t=t_s, regularly distributed during each fatigue test. As stated above, 1000 infrared images were acquired at each time t_s and then processed according to Eq. (8a). Some typical radial temperature profiles evaluated at θ=0° are shown in Fig. 4a and 4b, in the case of ΔK=26 MPa·m$^{0.5}$ (i.e. K_{max}=13 MPa·m$^{0.5}$) and ΔK=60 MPa·m$^{0.5}$ (i.e. K_{max}=30 MPa·m$^{0.5}$), respectively. In the former case a temperature drop equal to about 0.8 K within a distance of 2.5 mm from the crack tip can be observed; conversely, in the latter case, the temperature decreases much more, being the drop about 3 K. Therefore, the signal-to-noise ratio is significantly higher in Fig. 4b than in Fig. 4a. To evaluate the first derivative at r=R (Eq. (6)), the temperature-distance data along the seven considered paths were fitted using a proper polynomial function, shown with a continuous line in Fig. 4.

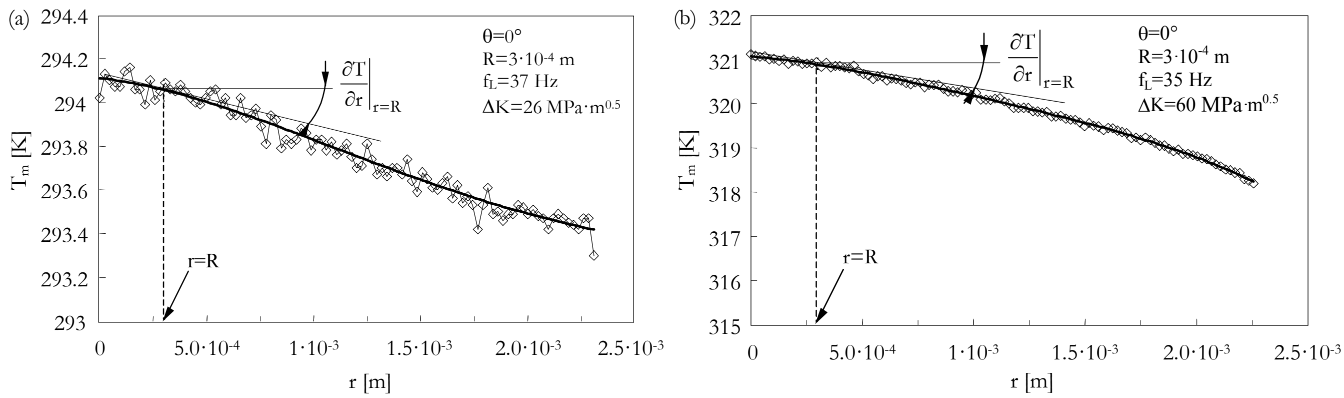

Figure 4: Typical radial temperature profiles measured during the tension-compression fatigue tests in the case of (a) $\Delta K=26$ MPa·m$^{0.5}$ and (b) $\Delta K=60$ MPa·m$^{0.5}$.

ENERGY PER CYCLE AVERAGED IN A VOLUME AT THE CRACK TIP

Fig. 5a, 5b and 5c show the specific thermal flux h at the different points along the boundary of V (Fig. 1) for specimen V_3, V_4 and V_5, respectively, using $\lambda=16$ W/(m·K) [8]. Finally, Fig. 5d shows, as an example, the specific energy flux per cycle q, obtained simply dividing h by the load test frequency. In the authors' opinion, for the material and the experimental conditions analysed in the present paper, a reasonably accurate evaluation of the heat power can be achieved by considering ΔK values higher than 25 MPa·m$^{0.5}$ ($K_{max}>12.5$ MPa·m$^{0.5}$).

Having in hand the specific thermal flux h evaluated at different angles θ of the boundary of V, numerical integration was performed according to Eq. (6). To evaluate the errors due to the discretisation, Eq. (6) was solved by dividing the 360° angle starting from a minimum of 4 intervals ($\Delta\theta=90°$) to a maximum of 24 ($\Delta\theta=15°$). A 0.51% variation on results was found by using 8 as compared to 24 intervals. Therefore, 8 intervals ($\Delta\theta=45°$) were adopted in numerical calculations. Finally, the energy per cycle averaged in the volume V, Q*, was evaluated by means of Eq. (7b). Results are listed in Tab. 1 and it can be seen that Q* increases as ΔK increases. It should be noted that ΔK are elastically calculated, independently on plastic zone size evaluations.

V_3 specimen		V_4 specimen		V_5 specimen	
ΔK [MPa·m$^{0.5}$]	Q* [MJ/m^3 cycle]	ΔK [MPa·m$^{0.5}$]	Q* [MJ/m^3 cycle]	ΔK [MPa·m$^{0.5}$]	Q* [MJ/m^3 cycle]
26.3	0.813	31.5	1.21	28.5	0.581
26.8	0.504	36.7	1.47	30.3	1.80
28.4	0.655	42.0	1.55	32.9	1.91
31.2	0.727	78.7	4.64	36.9	2.18
35.6	0.829	98.0	5.19	40.6	1.93
45.2	1.02			45.7	2.60
49.6	1.32			53.2	2.99
55.3	1.33			60.1	4.00
64.1	3.28			66.9	5.96

Table 1: Q* values calculated for different specimens at different ΔK values.

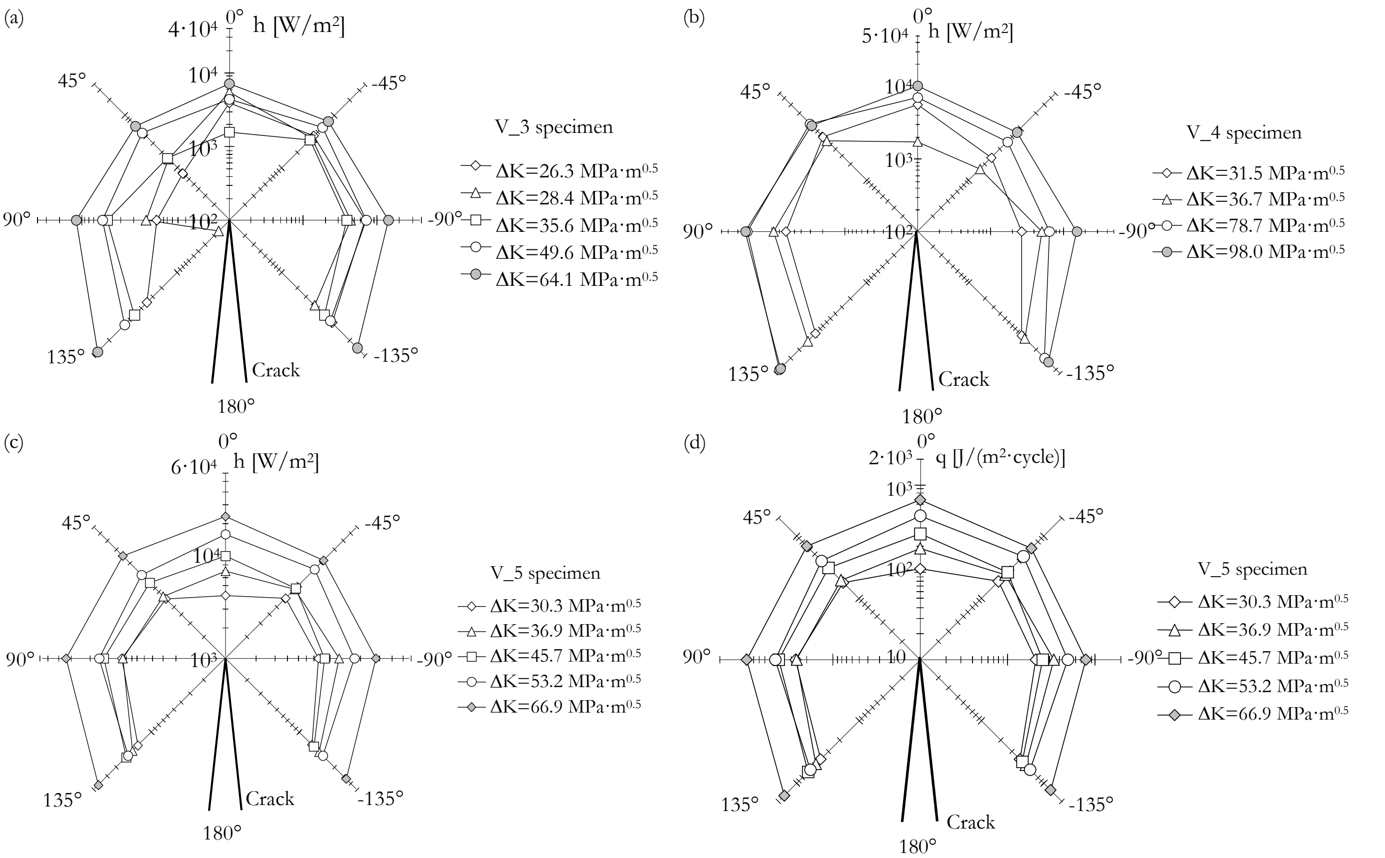

Figure 5: Distribution of the thermal flux *h* along the boundary of the control volume for different θ angles for (a) V_3, (b) V_4 (c) V_5 specimen and (d) and corresponding energy flux per cycle *q* of V_5 specimen.

COMPARISON BETWEEN EXPERIMENTAL AND THEORETICAL TEMPERATURES CLOSE TO THE CRACK TIP

An analytical solution is available in order to evaluate the time-dependent temperature field in the case of a homogeneous and isotropic infinite plate with a time-independent heat generation h_L distributed along a line in the thickness direction [18]. At the time t=0 when the heat generation starts, the temperature is supposed homogeneous and equal to T_0. Between time t=0 and t, the temperature variation $\Delta T(r,t)=T(r,t)-T_0$ can be expressed by Eq. (11) [18]:

$$\Delta T(r,t) = \frac{h_L}{4\pi\lambda} \cdot Ei\left(\frac{r^2}{4 \cdot \frac{\lambda}{\rho \cdot c} \cdot t}\right) \tag{11}$$

where Ei is the integral exponential function given by $Ei = \int_x^\infty e^{-u}/u \cdot du$ and x= $r^2 \Big/ \left(4 \cdot \frac{\lambda}{\rho \cdot c} \cdot t\right)$.

Since the major source of heat power is the cyclic plastic zone, the linear heat generation h_L was applied in its centre, according to [3]. Fig. 6a shows the cyclic plastic zone idealised as a circle having radius r_p. According to Irwin [20], the cyclic plastic zone radius in the plane stress condition is equal to:

$$r_p = \frac{1}{2\pi} \cdot \left(\frac{\Delta K}{2 \cdot \sigma'_{p,02}}\right)^2 \tag{12}$$

where $\sigma'_{p,02}$ is the material cyclic proof stress. For the AISI 304L steel material analysed in this paper, ρ=7940 kg/m^3, c=507 J/(kg·K) [19], $\sigma'_{p,02}$ =290 MPa [9].

With the aim to compare experimental results with the analytical solution Eq. (11), a dedicated fatigue tests was performed. A specimen containing a crack as long as half the width (i.e. the ligament length was about 23 mm according to Fig. 2) was installed in the fatigue machine to allow for thermal equilibrium with the surroundings so that the homogeneous temperature T_0 could be measured. Then the fatigue test was started with f_L=37 Hz and the load was adjusted to apply a linear elastic stress intensity factor range equal to ΔK=36.9 MPa·m$^{0.5}$; therefore r_p is equal to 6.44·10^{-4} m according to Eq. (12). The temperature field as well as the signal coming from the load cell were registered synchronously by the infrared camera using a sampling rate f_{acq}=200 Hz. To disregard the thermoelastic temperature oscillations superimposed to the mean temperature evolution T_m, which are not taken into account in Eq. (11), an infrared image captured at a time t=t* was considered, when the applied force was close to zero.

(a) (b)

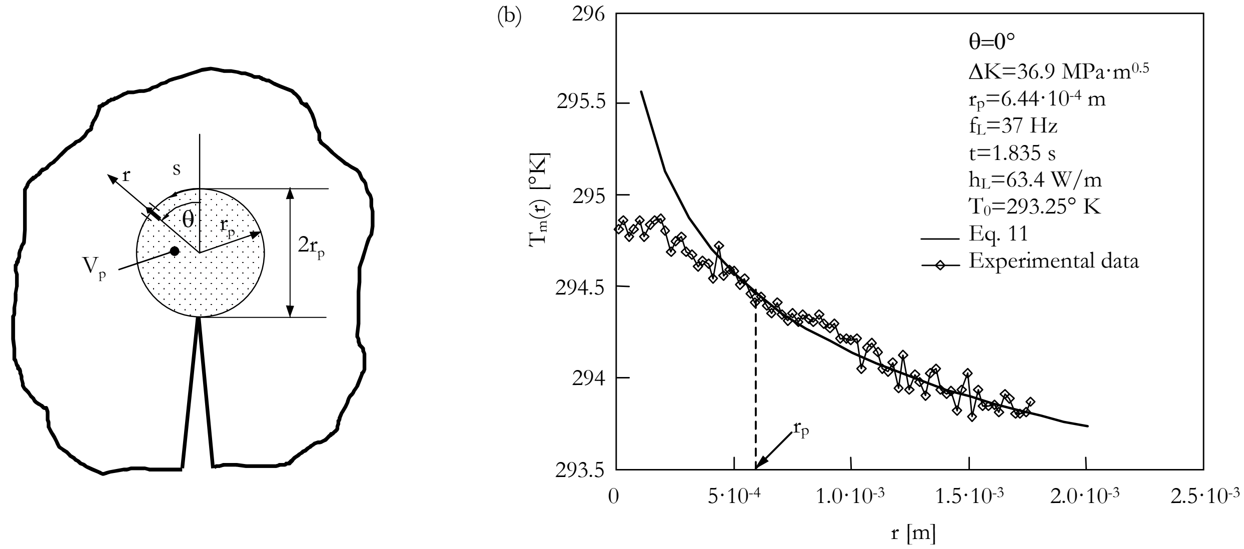

Figure 6: a) Cyclic plastic zone V_p and (b) comparison between experimental and theoretical radial temperature profile.

Fig. 7 shows the evolution of the temperature averaged inside the plastic zone V_p, T*(t), defined as:

$$T^*(t) = \frac{1}{V_p} \cdot \int_{V_p} T(t) \cdot dV_p \rightarrow \cong \frac{\sum_{i=1}^{n_{pixel}} T_i(t)}{n_{pixel}} \quad (13)$$

where n_{pixel} is the number of pixel inside the cyclic plastic zone size V_p. Fig. 7b shows the enlarged view of the "detail A" of Fig. 7a, where the thermoelastic effect superimposed to the mean temperature evolution T^*_m can be appreciated. Considering the radial temperature profiles that have been measured at t*=1.835 s (the applied force was approximately zero at this time), the total heat generated inside the cyclic plastic zone V_p was calculated according to Eqs (5) and (6). To evaluate the last contribution on the right hand side of Eq. (5) (the internal energy contribution), a linear fit of T* in a time window equal to 1s (Fig. 7b) was done and the slope of $T^*_m(t)$ was considered. After that, the constant heat generation per unit thickness h_L to input in Eq. (11) was calculated as:

$$h_L = \frac{1}{z} \cdot \int_{V_p} H_{gen} \cdot dV_p \quad (14)$$

and resulted equal to 63.0+0.4=63.4 W/m, where the first contribution is the conduction and the second is the internal energy term. Fig. 6b shows a comparison between the temperature field evaluated according to Eq. (11) and the experimental data for θ=0°. According to [2], it can be seen that outside the cyclic plastic zone the measured temperature field is in good agreement with that evaluated under the hypothesis of linear heat generation, which Eq. (11) is based on.

Inside the cyclic plastic zone differences are more pronounced because heat generation is actually distributed inside V_p, while in Eq. (11) it has been lumped to the centre of the cyclic plastic zone.

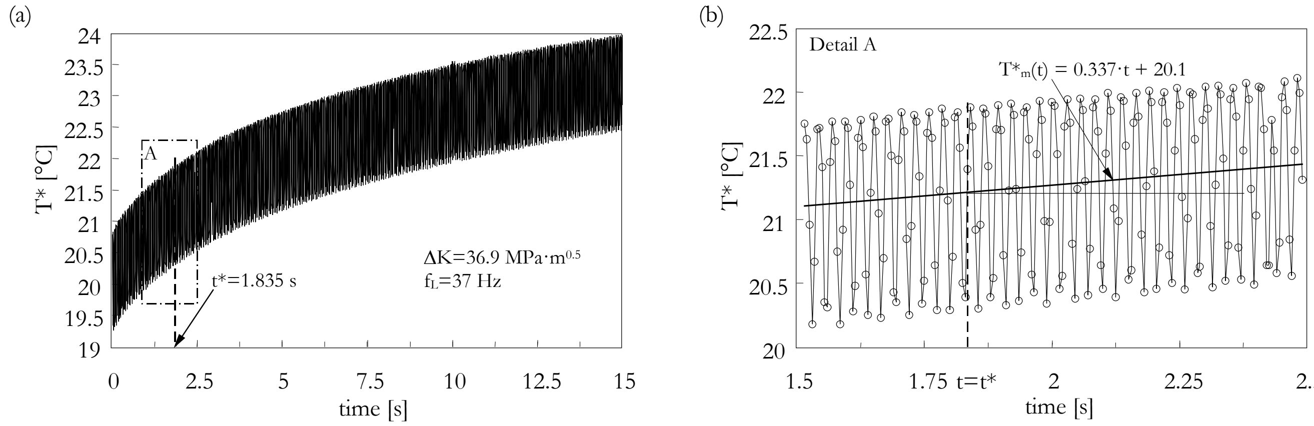

Figure 7: a) Temperature evolution during a fatigue test and b) enlarged view of detail A

DISCUSSION

As stated above, Eq (6) was derived under the assumption that the energy dissipated by convection and radiation is negligible, i.e. $H \cong H_{cd}$. The specific thermal flux power extracted by natural convection h_{cv} and that dissipated by radiation h_{ir} are given by

$$h_{cv}(r,\theta;t) = \alpha \cdot \left(T\left(r,\theta;t\right) - T_\infty\right) \tag{15a}$$

$$h_{ir}(r,\theta;t) = \kappa \cdot \sigma_n \cdot \left(T^4\left(r,\theta;t\right) - T_\infty^4\right) \tag{15b}$$

where α is the heat transfer coefficient by convection, κ is the surface emissivity, σ_n the Stephan–Boltzmann constant and T_∞ the room temperature. By considering, as an example, the experimental conditions of V_5 specimen and ΔK=40.6 MPa·m$^{0.5}$, the mean temperature averaged inside V, T^*_m, was equal to 28.1°C, T_∞=19°C, κ=0.92 [8] and f_L=35 Hz. By assuming a reasonable heat transfer coefficient under the hypothesis of natural convection on the order of α=10 W/(m^2 K) and considering that $S_{cv}=S_{ir}=2\cdot\pi R^2$, Q^*_{cv} and Q^*_{ir} can be calculated by means of Eqs 15 and 7a:

$$Q^*_{cv} = \frac{h_{cv} \cdot S_{cv}}{f_L \cdot V} \tag{16}$$

The result is Q^*_{cv}=867 J/(m^3·cycle) and Q^*_{ir}=472 J/(m^3·cycle), respectively, that are four order of magnitude lower than the relevant Q* values reported in Tab. 1, that take into account only the conduction term.

CONCLUSIONS

A theoretical framework has been defined to estimate the specific heat energy per cycle averaged in a defined volume surrounding the tip of a propagating crack, Q*. A two-dimensional thermal and structural problem has been considered. Experimental tests were executed on AISI 304L stainless steel cracked specimens subjected to push-pull fatigue loads and the Q* parameter has been determined starting from temperature measurements performed in the vicinity of the crack tip by means of an infrared camera. With reference to the material and experimental equipment available in the present paper, a reasonably accurate estimation of Q* was possible only for K_{max}>13 MPa·m$^{0.5}$. The experimental temperatures close to the crack tip were compared successfully with an analytical solution available in the literature.

ACKNOWLEDGEMENTS

This work was carried out as a part of the project CODE CPDA145872 of the University of Padova. The Authors would like to express their gratitude for financial support.

REFERENCES

[1] Klingbeil, N.W., A total dissipated energy theory of fatigue crack growth in ductile solids. Int J Fatigue, 25 (2003) 117-128.
[2] Ondracek, J., Materna, A., FEM evaluation of the dissipated energy in front of a crack tip under 2D mixed mode loading condition. Procedia Materials Science, 3 (2014) 673-678. DOI: 10.1016/j.mspro.2014.06.111.
[3] Ranc, N., Palin-Luc, T., Paris, P.C., Thermal effect of plastic dissipation at the crack tip on the stress intensity factor under cyclic loading. Eng Fract Mech, 78 (2011) 961-972. DOI: 10.1016/j.engfracmech.2010.11.010.
[4] Ranc, N., Palin-Luc, T., Paris, P.C., Saintier, N., About the effect of plastic dissipation in heat at the crack tip on the stress intensity factor under cyclic loading, Int J Fatigue, 58 (2014) 56-65. DOI: 10.1016/j.ijfatigue.2013.04.012.
[5] Bär, J., Seifert, S., Investigation of energy dissipation and plastic zone size during fatigue crack propagation in a high-alloyed steel, Procedia Materials Science, 3 (2014) 408-413. DOI: 10.1016/j.mspro.2014.06.068.
[6] Plekhov, O., Fedorova, A., Kostina, A., Panteleev, I., Theoretical and experimental study of strain localization and energy dissipation at fatigue crack tip, Procedia Materials Science, 3 (2014) 1020-1025. DOI: 10.1016/j.mspro.2014.06.166.
[7] Fedorova, A.Yu., Bannikov, M.V., Plekhov O.A., Infrared thermography study of the fatigue crack propagation, Fracture and structural integrity, 21 (2012) 46-53. DOI: 10.3221/IGF-ESIS.21.06.
[8] Meneghetti, G., Analysis of the fatigue strength of a stainless steel based on the energy dissipation, Int J Fatigue, 29 (2007) 81–94, DOI:10.1016/j.ijfatigue.2006.02.043.
[9] Meneghetti, G., Ricotta, M., The use of the specific heat loss to analyse the low- and high-cycle fatigue behaviour of plain and notched specimens made of a stainless steel, Eng. Fract. Mech. 81 (2012) 2–17. DOI: 10.1016/j.engfracmech.2011.06.010
[10] Meneghetti, G., Ricotta, M., Atzori, B., A synthesis of the push-pull fatigue behaviour of plain and notched stainless steel specimens by using the specific heat loss, Fatigue Fract. Engng. Mater. Struct., 36 (2013) 1306-1322. DOI: 10.1111/ffe.12071.
[11] Meneghetti, G., Ricotta, M., Atzori, B., Experimental evaluation of fatigue damage in two-stage loading tests based on the energy dissipation, Proc IMechE Part C: J Mechanical Engineering Science, 229 (2015) 1280-1291. DOI: 10.1177/0954406214559112.
[12] Peterson, R. E., Notch sensitivity, in: G. Sines and J. L. Waisman (Eds.) Metal Fatigue, MacGraw-Hill, New York, (1959) 293-306.
[13] Neuber, H., Über die Berücksichtigung der spannungskonzentration bei festigkeitsberechnungen. Konstruction, 20 (1968) 245-251.
[14] Ellyin, F., Fatigue damage, crack growth and life prediction, Chapman & Hall, London, (1997).
[15] Pandey, K.N., Chand, S., Deformation based temperature rise: a review, Int J Pres Ves Pip, 80 (2003) 673-687.
[16] Charkaluk, E., Constantinescu, A., Dissipation and fatigue damage. Proceedings of the Fifth International Conference on Low Cycle Fatigue LCF 5, Berlin, Germany, (2003).
[17] Plekhov, O.A., Panteleev, I.A., Naimark, O.B., Energy accumulation and dissipation in metals as a result of structural-scaling transitions in a mesodefect ensemble, Physical Mesomechanics, 10 (2007) 294-301.
[18] Carslaw, HS., Jaeger, JC, Conduction of heat in solids, Clarendon Press, Oxford, (1947).
[19] Atzori, B., Meneghetti, G., Ricotta, M. Analysis of the fatigue strength under two load levels of a stainless steel based on energy dissipation, In: Bremand F, editor. Proceedings of the 14th International Conference on Experimental Mechanics ICEM 14, The European Physical Journal EPJ Web of Conferences, 6 (2010).
[20] Irwin, G.R., Linear fracture mechanics, fracture transition and fracture control, Eng Fract Mech, 1 (1968) 241-257.